Gravitational Waves and Merging Black Holes: Analyzing GW150914

Aidan A. Sirbu[1] and Katie N. Brown[1]

[1] *Western University*
1151 Richmond St,
London, ON N6A 3K7, Canada

ABSTRACT

The purpose of this investigation is to explore the properties of gravitational waves and the evolution of black hole mergers. This is performed in the context of GW150914 using a classical model with minimal general relativistic corrections. The gravitational wave event was detected by the LIGO on September 14, 2015 at 09:50:45 UTC. The source of GW150914 has been established in previous work to be a binary black hole merger. The determination of the individual masses is based on Newtonian and Keplerian dynamics. This investigation explores the effectiveness of classical physics in predicting the behaviour and characteristic masses of the black holes. Firstly, the relationship between gravitational wave frequency and black holes mass is determined. The gravitational wave frequency at merger is used to determine a total mass of $68.36M_{\odot}$. A linear regression of $f_{GW}^{-8/3}$ vs time is used to find a chirp mass of $27.81M_{\odot}$. Using varying ranges of frequency sample points, the masses of the two black holes were determined to lie in the ranges of $42.4M_{\odot}$ to $45.35M_{\odot}$ and $23.02M_{\odot}$ to $25.96M_{\odot}$. These classically determined masses are in moderate agreement with cited values deduced from general relativistic equations. Furthermore, Keplerian orbital equations as well as Newtonian mechanics are used to model the time-evolution of the system's orbital frequency, velocity and separation.

1. INTRODUCTION

Gravitational waves (GW's) are ripples in space-time caused by the acceleration of massive objects such as black holes and neutron stars orbiting one another. (Abbott et al. 2016b) The world's first and largest GW observatory is the Advanced Laser Interferometer Gravitational Wave Observatory (LIGO), with detectors in Livingston, Louisiana and Hanford, Washington. On September 14, 2015 at 09:50:45 UTC, LIGO directly detected the first GW, GW150914. The variations in length caused by this wave (at the location of the detectors) were 1000 times smaller than the nucleus of an atom (LIGO-Caltech 2021a). Yet, the signal was clear enough for scientists to quickly analyze it and deduce many characteristics of its source. This GW is believed to have been emitted by the inspiral and subsequent merger of a binary black hole system at a luminosity distance of 410 Mpc (Abbott et al. 2016a). As of January 2022, LIGO and its Italian counterpart Virgo have detected 50 confirmed GW's (Castelvecchi 2020). Thus far, all these detected GW's have been emitted in compact binary inspirals (merging black holes or neutron stars).

Studying GW's allows us to investigate some of the most elusive and important areas of astrophysics, such as expanding our understanding of general relativity (GR). Analyzing the sources of these waves sheds light on some of the densest objects and highest energy processes in our universe, such as supernovae and black hole mergers. GW's also allow us to study objects and events that cannot be observed through electromagnetic (EM) radiation (LIGO-Caltech 2021b). They are especially valuable as they do not experience the same level of distorting propagation effects that EM waves do as they travel through space.

The objective of this paper is to investigate the properties and behaviour of GW's and binary black hole mergers, particularly in the context of GW150914. The starting point is to explore the theoretical relationship between the total mass of a binary black hole system and the frequency of gravitational waves emitted in its merger. We then process and analyze the GW150914 signal to determine the initial individual masses of the black holes. Finally, we use this result to simulate the time-evolution of the orbital frequency, velocity and separation of the system throughout the inspiral.

This implications of this investigation lie in the efficacy of Newtonian and Keplerian dynamics being used to predict the inspiral of a binary black hole system. The GR considerations are kept at a minimum. Though it

is well established that the merger and ringdown phases of the black holes can only be accurately modelled with the use of GR, the paper explores the accuracy in predicting both the behaviour leading up to it, as well as the characteristic masses. Results are compared to cited values obtained through advanced numerical relativistic simulations and GR methods.

2. METHODS

2.1. *Investigating the Relationship Between Gravitational Wave Frequency and Black Hole Mass*

The starting point of this investigation is to explore the relationship between the mass of a binary black hole system and the frequency of the gravitational waves emitted in the system's coalescence. In order to derive a relationship between gravitational wave frequency and the system's mass, begin with the Newtonian orbital solution

$$\frac{1}{r} = \frac{GM_{tot}}{h^2}(1 + e\cos\phi). \tag{1}$$

Here, r is the instantaneous distance between the two bodies (assumed to be point masses), e is the orbit's eccentricity, h is the total angular momentum, and M_{tot} is the total mass of the system, $M_{tot} = m_1 + m_2$. Assuming the orbits to be circular, $e = 0$ and $h = rv_\phi$. This equation thus becomes

$$\frac{1}{r} = \frac{GM_{tot}}{r^2 v_\phi^2}. \tag{2}$$

Substituting angular velocity in terms of angular frequency, as $v_\phi = r\omega$, then rearranging yields

$$\omega = \sqrt{\frac{GM_{tot}}{r^3}}. \tag{3}$$

At the time of the merger, the distance between the two bodies is the product of the compactness ratio $\mathcal{R}$ and the sum of the Schwarzschild radii of the two bodies,

$$\begin{aligned} r_m &= \mathcal{R}(r_{sc,1} + r_{sc_2}) \\ &= \mathcal{R}\left(\frac{2Gm_1}{c^2} + \frac{2Gm_2}{c^2}\right) \\ &= \mathcal{R}\frac{2GM_{tot}}{c^2}. \end{aligned} \tag{4}$$

The angular frequency at the time of the merger ω_m is thus

$$\omega_m = \frac{1}{\sqrt{8}}\frac{c^3}{\mathcal{R}^{3/2}GM_{tot}} \tag{5}$$

Due to the fact that at leading order, gravitational radiation is quadrupolar, which is symmetric under rotations by π about the orbital axis, the frequency of the gravitational waves is twice that of the orbit (Abbott et al. 2016b):

$$f_{GW,m} = \frac{2\omega_m}{2\pi}. \tag{6}$$

Thus, the frequency of the gravitational waves at the time of the merger is

$$f_{GW,m} = \frac{1}{2\sqrt{2}}\frac{c^3}{\pi GM_{tot}\mathcal{R}^{3/2}}. \tag{7}$$

Note that this is taken to be the frequency at which the waveform has the greatest amplitude (Abbott et al. 2016b).

In order to visualize this relationship, the expected frequency of gravitational waves emitted by mergers of black hole systems of various sizes is plotted in figure 1. The frequency range detectable by the LIGO detectors is also shown, and equation 7 is used to determine the range of black hole mergers observable by LIGO.

2.2. *Signal Processing*

In order to begin working with the GW150914 data (LIGO Scientific Collaboration 2016), a plethora of signal processing techniques must be applied to filter the noise. It is known that the event occurred at GPS time 1126259462. While various samples of the GW150914 data are available, for the purpose of this analysis the 32 second data sampled at 4096 Hz is used. In general, LIGO strain data includes gaps when the detectors are considered to be measuring periods of poor data quality (Abbott et al. 2020). The determination of data quality depends on a variety of factors which are made available for the public (Abbott et al. 2021). The 4096 seconds of data was specifically chosen by GWOSC to include no such gaps and therefore provides a simplification to the process. The 32 second version provides a further condensation of the data. Since the GW itself was only detected over the course of milliseconds, the 32 second data is more than sufficient. Furthermore, 4096 Hz is chosen instead of the available 16384 Hz to reduce disk space and memory required. The down-sampled 4096 Hz data was also determined to be entirely sufficient for signals with no frequency content above the Nyquist frequency of 2048 Hz, such as GW150914 (Abbott et al. 2021).

The exact location of the GW within both the spatial and frequency domains of the detector data is predetermined. Portions of the Python code is re-purposed

from GWOSC (2017). The signal is filtered in the time domain, using bandpassing to reveal the signal in the frequency band [40Hz, 300Hz]. The notching of spectral lines is also used to remove the noise sources from the data.

A theoretical numerical relativity (NR) template was generated by GWOSC with parameters from the GW150914 detection paper (Abbott et al. 2016a). The NR template produced a theoretical waveform expected to be detected from two merging black holes of ∼36 and ∼29 solar masses into ∼62 solar masses at a distance of 410 Mpc. The template is compared to the signal data in order to further reduce noise near zero crossings as described in section 2.3.

2.3. *Determining Total and Chirp Mass*

Firstly, the analysis of the GW frequency is constrained to begin at T-0.10s[1] in order for the first zero crossing to be followed by coherent signal that is distinguishable from noise. The signal's zero crossings are used to deduce the frequency of the GW with

$$f_{GW} = \frac{1}{2\delta t_{cross}}, \tag{8}$$

where δt_{cross} is the time interval between consecutive zero crossings. For times previous to T-0.05s, noise appears to affect the signal in a manner that produces too many zero crossings in regions where the frequency should be low. The time values of the zero crossings in these regions are averaged to further filter out noise. In order to determine which zero crossings are averaged, the NR waveform is used to determine the number of expected zero crossings and their approximate positions.[2] The averaging is performed in regions with a higher occurrence of zero crossings than predicted by the NR template. The frequency at merger, $f_{GW,m}$, is deduced from the time interval between consecutive zero crossings where the signal is at maximum amplitude. Equation (7) is then used to find M_{tot} with $\mathcal{R}$ taken to be 1.7.

Compactness ratio is defined as the closest orbital separation of the black holes before merger divided by the sum of their Schwarzschild radii. The masses of the black holes are determined using an assumed compactness ratio of 1.7 which was determined in Abbott et al. (2016b). This compactness ratio was reached by using a total mass of $70M_{\odot}$ and an orbital separation of 350km at merger. In order to justify the use of $\mathcal{R} = 1.7$, an equilibrium function approach is taken. The total mass, chirp mass, and GW frequency at merger deduced using $\mathcal{R} = 1.7$ are used to recalculate the compactness ratio. The new compactness ratio is then used to recalculate total mass using equation (7). This process is then iterated with a tolerance limit on $\Delta\mathcal{R}$ of 1×10^{-15} as the termination criterion. The compactness ratio determined through this process is within 0.04% difference of 1.7 and so determined to be an inadmissible difference. Hence, $\mathcal{R} = 1.7$ is a justifiable value to use for the masses involved in this investigation.

The next step is to use the previously calculated frequency values to estimate the system's chirp mass M_{ch}, which is defined in terms of the individual black hole masses by

$$M_{ch} = \frac{(m_1 m_2)^{3/5}}{(m_1 + m_2)^{1/5}}. \tag{9}$$

Equation 8 in Abbott et al. (2016b) gives the time evolution of the gravitational wave frequency as

$$f_{GW}^{-8/3}(t) = \frac{(8\pi)^{-8/3}}{5}\left(\frac{GM_{ch}}{c^3}\right)^{5/3}(t_c - t), \tag{10}$$

where t_c is the time of coalescence of the binary system. This is a linear function in t with a slope given by

$$\frac{df_{GW}^{-8/3}}{dt} = -\frac{(8\pi)^{-8/3}}{5}\left(\frac{GM_{ch}}{c^3}\right)^{5/3}. \tag{11}$$

Rearranging for the chirp mass in terms of this slope yields

$$M_{ch} = -\frac{c^3}{G}\left(\frac{5}{(8\pi)^{-8/3}}\frac{df_{GW}^{-8/3}}{dt}\right)^{3/5}. \tag{12}$$

In order to calculate the chirp mass, the measured frequencies are each raised to the power of $-\frac{8}{3}$. An array of corresponding time points is produced by taking the midpoint of each pair of zero-crossings. The `np.polyfit` function is used to produce a least squares linear fit to $f_{GW}^{-8/3}$ as a function of time. This linear function is plotted with the measured frequency points to illustrate the data fit (see figures 3 and 5). The slope of this function, $\frac{df_{GW}^{-8/3}}{dt}$, can then be used with equation (12) to determine the chirp mass. This procedure is performed for the original set of 12 frequency data points and a reduced set of 4 points.

[1] T being the the event time

[2] Refer to figure 4 for a visual representation.

2.4. *Determining Individual Masses*

Once the system's total and chirp masses are determined, it is simple to calculate the individual masses of the two black holes. Substituting $m_2 = M_{tot} - m_1$ into equation (12), which defines the chirp mass, produces the quadratic polynomial in m_1:

$$m_1^2 - M_{tot}m_1 + (M_{ch}^5 M_{tot})^{1/3} = 0. \quad (13)$$

The solutions to this equation are

$$m1, m2 = \frac{1}{2}M_{tot} \pm \frac{1}{2}\sqrt{M_{tot}^2 - 4(M_{ch}^5 M_{tot})^{1/3}}. \quad (14)$$

These are the individual masses of the two black holes.

2.5. *Time-Evolution of Orbital Frequency, Velocity and Separation*

This section of the investigation involves analytically calculating the time evolution of the orbit frequency, orbit velocity and the orbital separation of the binary black hole system responsible for GW150914. Firstly, we begin with equation (28) from (Abbott et al. 2016b) which describes the orbital frequency of the system as a first-order differential equation

$$\dot{\omega}^3 = \left(\frac{96}{5}\right)^3 \frac{\omega^{11}}{c^{15}}(GM_{ch})^5. \quad (15)$$

Upon integration, orbital angular frequency is determined to be

$$\omega = \left(\frac{5}{256\tau}\right)^{3/8}\left(\frac{GM_{ch}}{c^3}\right)^{-5/8}, \quad (16)$$

where $\tau = t_c - t$ and t_c is the time of coalescence. Furthermore, Kepler's third law states that the orbital separation is related to orbital angular frequency through:

$$r = \sqrt[3]{\frac{GM_{tot}}{\omega^2}}. \quad (17)$$

From this, one can directly obtain an expression for orbital separation with respect to time by substitution of equation (16) into (17):

$$r = G^{3/4}M^{1/3}\left(\frac{256\tau}{5}\right)^{1/4}\left(\frac{M_{ch}}{c^3}\right)^{5/12} \quad (18)$$

Next, one can substitute v_ϕ/ω and equation (16) into equation (17) and rearrange to obtain

$$v_\phi = M_{tot}^{1/3}\left(\frac{5G}{256\tau}\right)^{1/8}\left(\frac{M_{ch}}{c^3}\right)^{-5/24} \quad (19)$$

which describes the orbit velocity of the system. Note that these equations have been derived using Newtonian and Keplerian dynamics. These equations describe the inspiral of the binary black hole system up to a point in which GR considerations must be taken into account. More on this in section 3.5.

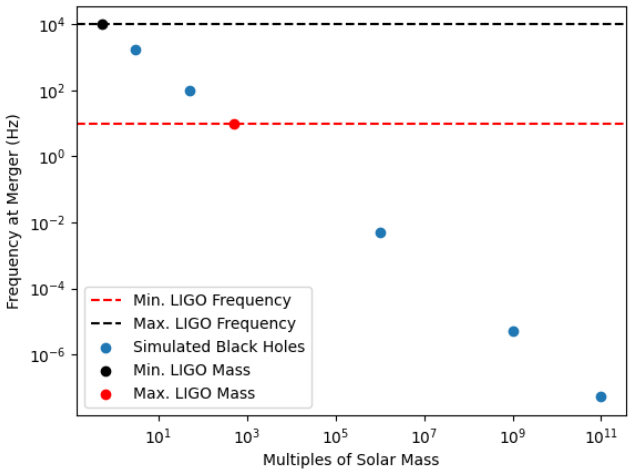

Figure 1: The estimated gravitational wave frequency emitted by mergers of binary black hole systems with varying *total* masses. The simulated black hole furthest to the top-left (blue point) corresponds to the least massive black hole ever identified (XTE J1650-500 at $3.8M_\odot$)(Orosz et al. 2004). The horizontal lines show the frequency range over which the LIGO detectors are capable of observing (10 Hz to 10 kHz)(Martynov et al. 2016). The black and red dots (at $0.52M_\odot$ and $515.41M_\odot$, respectively) depict the corresponding minimum and maximum total masses of merging black holes detectable by LIGO.

3. RESULTS

3.1. *Relationship Between Gravitational Wave Frequency and Black Hole Mass*

As predicted by equation (7), figure 1 illustrates that there is a reciprocal relationship between the mass of the binary system and the frequency of the gravitational waves emitted in its merger. It it clear that the more massive a pair of black holes, the lower the frequency. In fact, two supermassive black holes are estimated to emit gravitational waves with a frequency of 5.15×10^{-8} Hz, which corresponds to a wavelength of 0.61 light-years.

Figure 1 also shows the range of frequencies over which the LIGO detectors are able to observe: 10 Hz to 10 kHz. This corresponds to binary systems over a range from $0.52M_\odot$ to $515.41M_\odot$. Note that this lower mass limit is actually much lower than the smallest possible black hole mass (Abbott et al. 2016b).

3.2. *Signal Processing*

The signal obtained at both Livingston and Hanford LIGO detectors are plotted following signal processing

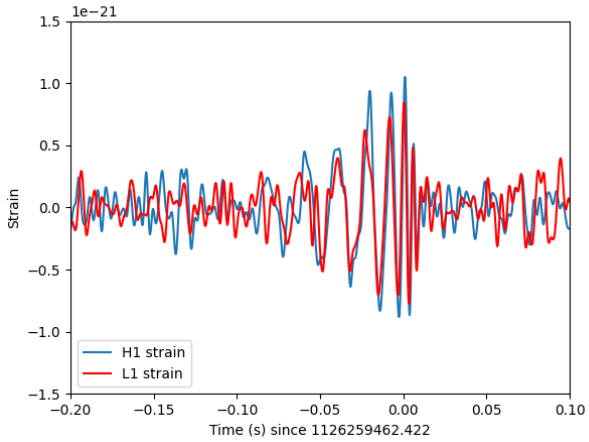

Figure 2: Strain data near GW150915 detected by Hanford (H1) and Livingston (L1) LIGO detectors. The time axis measures the time since GPS time 1126259462.42 corresponding to 09:50:45 UTC. The figure is recreated using the code made available by GWOSC (GWOSC 2017).

in figure 2. Prior to plotting, the Livingston data is shifted by 7ms as well as inverted. This is done in order to account for the time of flight delay between the detectors as well as their respective orientations (Abbott et al. 2016a). As one can observe, the data consists of what appears to be largely noise up until T-0.07. The signal then begins oscillating with increasing frequency and amplitude. The signal appears to peak in amplitude just after time zero, before then fading back into what appears to once again be mostly noise.

3.3. *Total and Chirp Mass*

As described in section 2.3, the total mass is arrived to by using the value obtained for the GW frequency at merger averaged between Hanford and Livingston, $f_{GW,m} = 150.87$ Hz, with equation (7). The estimated total masses are $66.71M_\odot$ for the Hanford detector and $70.02M_\odot$ for Livingston. These two are averaged to yield $68.36M_\odot$.

Figure 3 displays each measured frequency value, raised to the power of $-\frac{8}{3}$, plotted against time. Note that the zero crossings resulting from averaging the points displayed in figure 4 are used. Also plotted is the least squares linear fit that is produced to determine the approximate slopes of these lines. The slope values for the Hanford and Livingston data were found to be $df^{-8/3}/dt = -4.5 \times 10^{-4}$ and $df^{-8/3}/dt = -3.4 \times 10^{-4}$, respectively. These values are then used with equation

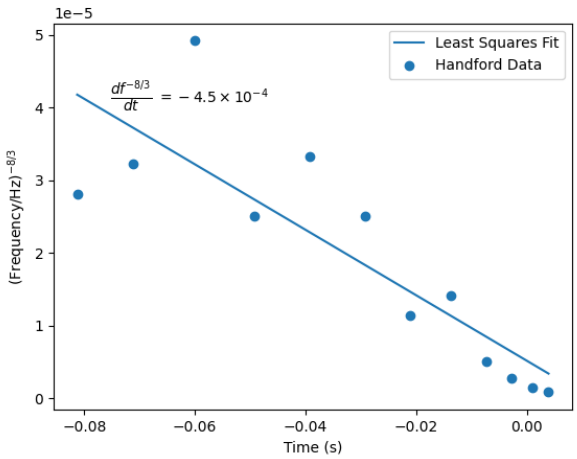

(a) Hanford detector data

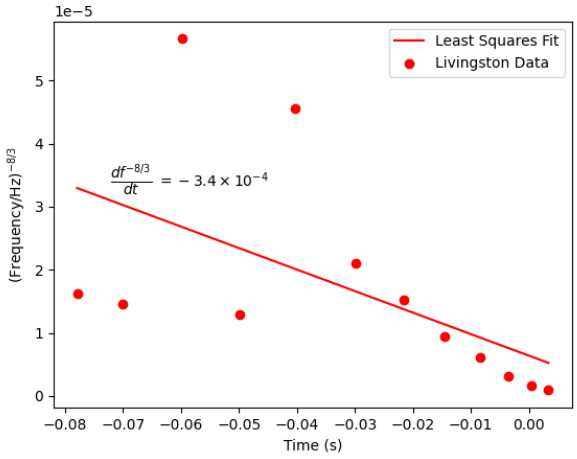

(b) Livingston detector data

Figure 3: The full sets of estimated frequencies (raised to the power of $-\frac{8}{3}$) plotted against time. Least squares linear fits are also shown, along with their slopes.

(12) to estimate chirp mass values of $30.13M_\odot$ and $25.49M_\odot$, from the H1 and L1 data, respectively. These values are averaged to find a final estimated chirp mass of $27.81M_\odot$.

As illustrated in figure 3, points further from the event time have larger residuals as they do not agree with the linear fit as closely. In order to mitigate this, the procedure is repeated for the limited set of frequency points calculated in section 3.3. This data and the resulting least squares linear fit are presented in figure 5. The slopes determined from this fit are $df^{-8/3}/dt = -3.8 \times 10^{-4}$ and $df^{-8/3}/dt = -4.5 \times 10^{-4}$ for the H1 and L1 data, respectively. These correspond

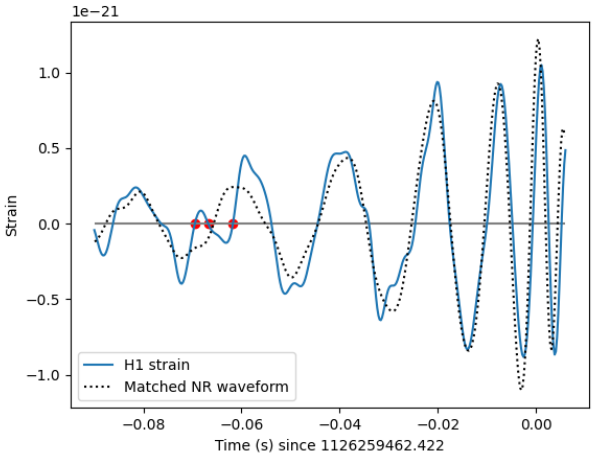

(a) Hanford detector data

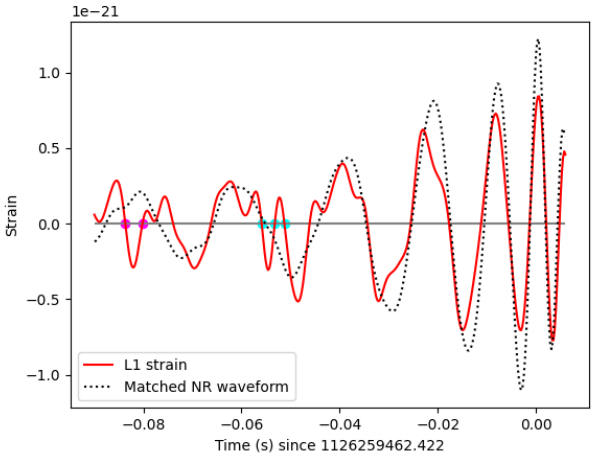

(b) Livingston detector data

Figure 4: GW150915 waveforms as measured by the H1 and L1 LIGO detectors. The matched NR waveform is used to determine the zero crossings that are averaged. In figure (a) the red points highlight three zero crossings that are averaged in order to yield only one crossing as matched by the NR waveform. In figure (b) the magenta and cyan points are averaged.

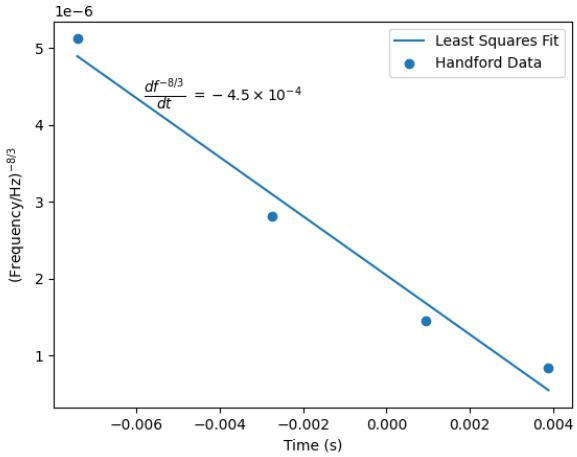

(a) Hanford detector data

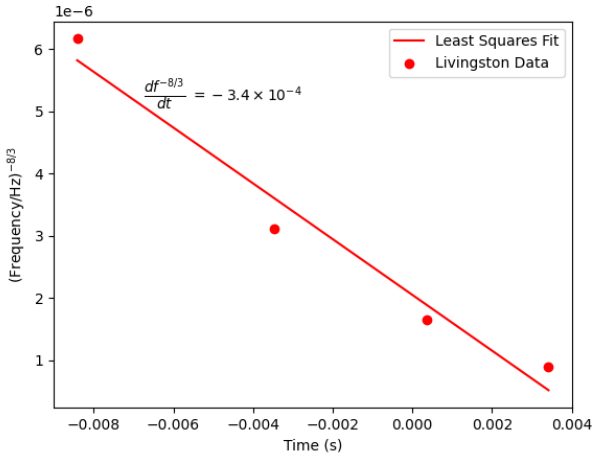

(b) Livingston detector data

Figure 5: Estimated frequencies (raised to the power of $-\frac{8}{3}$) plotted against time. Only the last four data points are shown here. Least squares linear fits are also shown, along with their slopes.

to chirp mass estimates of $27.4M_\odot$ and $30.0M_\odot$. These values are averaged to arrive at the final chirp mass estimate of $28.71M_\odot$.

3.4. *Individual Masses*

Inserting the values for total mass and chirp mass presented in section 3.3 into equation (14) gives estimates of the individual masses of the two black holes. Using the results from the complete set of frequency points, the estimated masses are $45.35M_\odot$ and $23.02M_\odot$. When the results from the final four frequency points are used, the masses are found to be $42.4M_\odot$ and $25.96M_\odot$. These values will be taken as the estimated range within which the masses will lie. The less massive black hole should fall between $23.02M_\odot$ and $25.96M_\odot$, while the larger should fall between $42.4M_\odot$ and $45.35M_\odot$. One should note that these ranges are not rigorously defined. The analysis of 4 and 12 frequency points can be argued to be somewhat arbitrary; sets of 5 and 11 point would have equally valid. The purpose this serves is to provide a rudimentary uncertainty range in the values and more importantly, to highlight the variation in results based on the number of frequency points sampled.

3.5. *Time-Evolution of Orbital Frequency, Velocity and Separation*

The time-evolution of the orbital frequency, velocity and separation are plotted for the binary black hole system in figure 6. As mentioned in section 2.5, Keplerian dynamics can only predict the inspiral of the binary black hole system up to a certain point. In order to determine that point, the Schwarzschild radii of each individual mass is first determined. Next, the orbital separation at merger is assumed to occur when the Schwarzschild radii of the black holes overlap. GR considerations of compactness are taken into account here. The sum of their Schwarzschild radii is multiplied by their compactness ratio.[3] From this, the time of merger is found and used to determine the orbital velocity and frequency at merger. One should note that the behaviour of each series above the dotted green line in figures 6(a) and 6(b) and below in 6(c) should be disregarded since the merger and ringdown phases can only be calculated in numerical relativity simulations not discussed here. The theoretical behaviour is plotted from half a second before the merger in order to accurately demonstrate the rapidly increasing frequency and velocity near merger. Furthermore, the determination of the theoretical orbital frequency at merger (shown in figure 6(b)) provides confidence in the experimental results in section 3.3. The average of the experimentally determined GW frequencies at merger from Livingston and Hanford is 150.87 Hz. Using equation (6), this experimental orbital frequency at merger is 473.97 $\frac{rad}{s}$ which is within a 3% error margin compared to the theoretical value of 487.93 $\frac{rad}{s}$. Furthermore, the theoretical value for orbital separation at merger is 333.2 km while that of orbital velocity is 1.62×10^8 m/s, approximately half the speed of light.

4. DISCUSSION

The discussion begins with a justification that GW150914 originates from the inspiral and coalescence of binary black holes. Firstly, the signal itself suggests that the source is a merger of two compact objects in a binary system. GR states that GW's are produced by accelerating masses. The nearly sinusoidal waveform seen in figure 2 indicates that the accelerating mass or masses are oscillating. Furthermore, the signal's behaviour of increasing frequency and amplitude up to a point in which it abruptly ceases and returns to noise at around T+0.2s suggests that it is caused by oscillating masses which eventually collide into one another. A

[3] The compactness ratio used is 1.7.

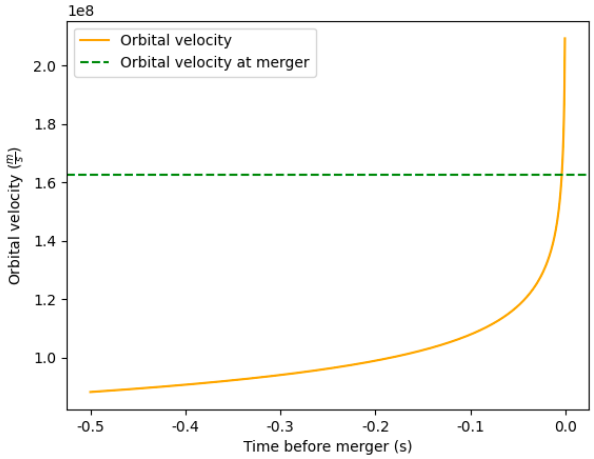

(a) Orbital velocity

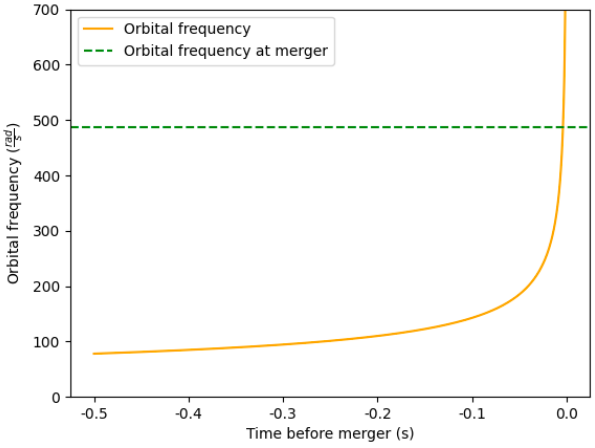

(b) Orbital frequency

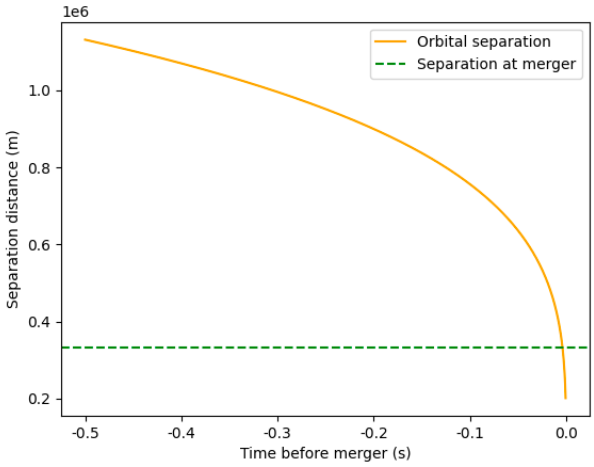

(c) Orbital separation

Figure 6: Analytical solutions of orbital velocity, frequency and separation of binary black hole system responsible for GW150914. The orange plots represent Keplerian solutions for the merging of the black holes. The green dotted line represents the approximate region where Keplerian dynamics no longer accurately predict behaviour.

system oscillating towards an equilibrium point would instead see a gradual decreases in frequency and amplitude instead. As discussed by Abbott et al. (2016b), GW's allow orbiting masses to shed their energy, acting as a damping force. This decreases their orbit and leads into an inspiral with eventual coalescence. All this evidence prompted for the construction of an analytical model of a compact binary inspiral. Note that none of the equations ((7), (12), and (14)) used to calculate the objects' masses assumed that these compact objects are black holes. The two objects are found to have masses of at least $23.02M_\odot$ and $42.4M_\odot$. The Tolman-Oppenheimer-Volkoff limit gives the maximum possible mass for a neutron star to be $2.7M_\odot$ (Moffat 2020). Similarly, the Chandrasekhar limit constrains white dwarf masses to no more than $1.4M_\odot$. Thus, the results of this investigation strongly suggest that the source of GW150914 is the inspiral of a binary black hole system.

Upon analysis of figure 1 it appears as though LIGO detectors possess a fairly limited range of black hole merger detection capability. This limitation however does not originate from its lower limit. As mentioned previously, the least massive black hole ever measured was well above the lower limit of LIGO detection. The most massive black hole mergers LIGO can detect are on the lower end of intermediate-mass black holes. Intermediate mass black holes range from $10^2M_\odot$ to $10^5M_\odot$ while the largest black holes LIGO can detect is on the order of $10^2M_\odot$[4]. (Green 2012).

To continue, as observed in figure 4, the NR waveform appears to reach a greater maximum amplitude than the signals detected from Hanford and Livingston. This, however, does not render the method of mass determination any less valid since the NR waveform is used to average zero crossings which appear to be the product of noise. The approach taken in mass determination relies heavily on Newtonian and Keplerian dynamics. The inspiral of the black holes is assumed to be circular up to the point of merger and therefore follows a Keplerian orbit. The masses of the black holes are determined to lie in the ranges of $42.4M_\odot$ to $45.35M_\odot$ and $23.02M_\odot$ to $25.96M_\odot$. Abbott et al. (2016a) also analyzed GW150914 using general relativistic simulations and obtained values of $36^{+5}_{-4}M_\odot$ and $29^{+4}_{-4}M_\odot$. The lower mass range determined in this investigation lies within the range of uncertainty of that of Abbott et al. (2016a) however the upper mass range does not. Abbott et al. (2016a) also estimate that the total energy radiated through GW's during this inspiral is 5.3×10^{47} J or, equivalently, $3.0M_\odot c^2$. This mass loss may be a factor in the upper mass determination lying outside of the range of uncertainty. Furthermore, Abbott et al. (2016a) performed the mass analysis on the matched NR waveform using general relativistic considerations which more accurately model the merger and ringdown phases of the black holes. An interesting implication of this investigation is the power behind Newtonian mechanics. The only relativistic consideration used (aside from the averaging based on the NR waveform) is the compactness ratio based on the Schwarzschild radii of the black holes. In spite of the approximations used, the resulting masses are within a very close range of those predicted with relativistic simulations.

The next task of this investigation lies in analytically solving for the orbital frequency, velocity and separation. In order to do achieve this, Newtonian and Keplerian mechanics were once again used. The resulting models represented in figure 6 appear to predict the general trend of the merger. Each quantity behaves as expected with both orbital velocity and frequency increasing rapidly near the point of merger (shown by the green dotted line) while the orbital separation rapidly decreasing. While an argument can be made that the theoretical predictions match the analysis of the data, both were obtained using purely classical considerations, save the compactness ratio. The overall intent of modelling these quantities is to make a case that Newtonian and Keplerian dynamics can and do predict general behaviour up until the point of merger.

5. CONCLUSIONS

The purpose of this investigation is to explore the properties of gravitational waves and the evolution of black hole mergers, especially in the context of GW150914. Firstly, we apply Newtonian dynamics with some simple GR corrections to construct a theoretical relationship between GW frequency and the mass of the binary system whose merger is emitting the GW. We find a reciprocal dependence on total mass; the more massive two black holes are, the lower frequency GW's they will emit in their merger. This has implications for LIGO, whose detectors are only capable of observing frequencies as small as 10 Hz. This emphasizes the im-

[4] Since the frequency of a GW reaches its *maximum* at the time of merger, LIGO would not actually likely be able to detect a GW from merging black holes with masses as large as $10^2M_\odot$; the majority of the waveform would lie outside its sensitivity range. The true upper mass limit detectable by LIGO is expected to be smaller than this value.

portance of developing a network of GW observatories that are able to detect waves over a greater frequency range.

The strain data from GW150514 is processed through whitening and bandpassing to reduce noise and produce a clear signal. The signal is then compared to a numerical relativity template to further distinguish between the waveform and noise. Simple computational analysis is performed to estimate the frequency of the signal at each point. The frequency at merger (at the point of highest GW amplitude) is used to estimate a total system mass of $68.36M_{\odot}$. The overall time-evolution of the frequency values is then used to estimate a chirp mass value between $27.81M_{\odot}$ and $28.71M_{\odot}$. These results are consistent with those determined by Abbott et al. (2016a), who performed analysis using a more complex GR-based model supported with advanced statistical techniques. Based on these results, we determine that the initial masses of the two individual black holes should be between $23.02M_{\odot}$ and $25.96M_{\odot}$, $42.4M_{\odot}$ and $45.35M_{\odot}$.

Finally, we use these mass results to analytically model the time-evolution of the frequency, velocity and separation of the orbit. The results are as expected: the orbital velocity and frequency increase sharply as the two black holes orbit increasingly close together. The point of merger is defined as an orbital separation of 333.2 km . At this point in time, the orbital velocity and frequency were estimated to be 1.62×10^8 m/s and 473.97 $\frac{rad}{s}$, respectively.

Analyses into GW's and their sources are an incredibly valuable tool for astrophysicists to study the nature and dynamics of gravity and compact objects. Using the data from the 50 GW's detected by LIGO thus far, astrophysicists have been able to estimate how the frequency of black hole mergers has changed throughout the evolution of the universe (Castelvecchi 2020). They have also gained valuable insight into the mass-distribution of the black holes undergoing these mergers. GW's may even allow for a more accurate determination of the Hubble Constant which characterizes the rate of expansion of the universe (Castelvecchi 2018). We should continue to invest in the development of GW detection technology to improve our understanding of such important areas of astrophysics.

APPENDIX

A. ACKNOWLEDGMENTS

This research has made use of data or software obtained from the Gravitational Wave Open Science Center (gw-openscience.org), a service of LIGO Laboratory, the LIGO Scientific Collaboration, the Virgo Collaboration, and KAGRA. LIGO Laboratory and Advanced LIGO are funded by the United States National Science Foundation (NSF) as well as the Science and Technology Facilities Council (STFC) of the United Kingdom, the Max-Planck-Society (MPS), and the State of Niedersachsen/Germany for support of the construction of Advanced LIGO and construction and operation of the GEO600 detector. Additional support for Advanced LIGO was provided by the Australian Research Council. Virgo is funded, through the European Gravitational Observatory (EGO), by the French Centre National de Recherche Scientifique (CNRS), the Italian Istituto Nazionale di Fisica Nucleare (INFN) and the Dutch Nikhef, with contributions by institutions from Belgium, Germany, Greece, Hungary, Ireland, Japan, Monaco, Poland, Portugal, Spain. The construction and operation of KAGRA are funded by Ministry of Education, Culture, Sports, Science and Technology (MEXT), and Japan Society for the Promotion of Science (JSPS), National Research Foundation (NRF) and Ministry of Science and ICT (MSIT) in Korea, Academia Sinica (AS) and the Ministry of Science and Technology (MoST) in Taiwan.

REFERENCES

Abbott, B., Abbott, R., Abbott, T., et al. 2016a, Physical Review Letters, 116, doi: 10.1103/physrevlett.116.061102

Abbott, B. P., Abbott, R., Abbott, T. D., et al. 2016b, Annalen der Physik, 529, 1600209, doi: 10.1002/andp.201600209

Abbott, B. P., et al. 2020, Class. Quant. Grav., 37, 055002, doi: 10.1088/1361-6382/ab685e

Abbott, R., Thomas D. Abbott, Sheelu Abraham, et al. 2021, SoftwareX, 13, 100658, doi: https://doi.org/10.1016/j.softx.2021.100658

Castelvecchi, D. 2018, Nature, 556, doi: https://doi.org/10.1038/d41586-018-04157-6

—. 2020, Nature, 523, doi: https://doi.org/10.1038/d41586-020-03047-0

Green, J. E. 2012, Nature Communications, 3, doi: https://doi.org/10.1038/ncomms2314

GWOSC. 2017, LOSC_Event_tutorial GWopenscience.org, GWOSC. https://www.gw-openscience.org/s/events/GW150914/LOSC_Event_tutorial_GW150914.html

LIGO-Caltech. 2021a, What are Gravitational Waves? https://www.ligo.caltech.edu/page/what-are-gw

—. 2021b, Why Detect Them? https://www.ligo.caltech.edu/page/why-detect-gw

LIGO Scientific Collaboration. 2016, Data release for event GW150914, Gravitational Wave Open Science Center, doi: 10.7935/K5MW2F23

Martynov, D., Hall, E., Abbott, B., et al. 2016, Physical Review D, 93, doi: 10.1103/physrevd.93.112004

Moffat, J. W. 2020, Modified Gravity (MOG) and Heavy Neutron Star in Mass Gap. https://arxiv.org/abs/2008.04404

Orosz, J. A., McClintock, J. E., Remillard, R. A., & Corbel, S. 2004, The Astrophysical Journal, 616, 376, doi: 10.1086/424892